Australian Government
Department of Defence
Defence Science and
Technology Organisation

Modelling Helicopter Radar Backscatter

R. Melino, C. Bourne and H.T. Tran

Electronic Warfare and Radar Division

Defence Science and Technology Organisation

DSTO–TR–2547

ABSTRACT

This paper presents a study on the simulation of the radar backscatter signal from a helicopter in which the helicopter rotors, the helicopter rotor hub and helicopter body are modelled by an ensemble of straight wires, rods and rectangular plates in various orientations. Despite the simplicity of exact solutions used here, which give a significant advantage of very low computational cost, very good agreement with real data can be achieved.

Published by

DSTO Defence Science and Technology Organisation
PO Box 1500
Edinburgh, South Australia 5111, Australia

Telephone: (08) 7389 5555
Facsimile: (08) 7389 6567

AR No. 014–993
June, 2011

APPROVED FOR PUBLIC RELEASE

Modelling Helicopter Radar Backscatter

Executive Summary

Given the relatively high costs of obtaining real radar data of targets of interest, and the high computational costs of high-fidelity numerically intensive simulation techniques, a 'fast and easy' tool for generating radar signals that closely simulate real helicopter returns is a desirable capability that can greatly aid the research and development of algorithms for the detection and classification of helicopter targets. We are reporting the development and performance of such a tool.

Models to mathematically describe the scattering from helicopters are investigated with the main scatterers being the rotors, rotor hub and helicopter body represented using simple objects such as straight wires, rods and rectangular plates at various orientations. By generating a composite model using these objects a complete representation of a helicopter can be built and a radar backscatter signal can be simulated.

This paper demonstrates the time and frequency characteristics associated with these simple models and the overall characteristics when objects are combined to form a composite model. When compared with real data the results show that the simulated and real signals are reasonably close, despite the very low computational cost.

THIS PAGE IS INTENTIONALLY BLANK

Contents

Figures

1 Introduction

Simulating the radar return from helicopters involves modelling the components that make up a helicopter. This includes the helicopter body and the rotating main rotor, which is made up of the rotor blade and rotor hub. These individual objects have specific shapes and give a specific radar return. The simulation of the radar returns from a combination of these structures can aid the research and development of detection and classification algorithms for helicopter targets by airborne pulsed Doppler radars.

There have been extensive studies on the modelling of rotating objects in the literature and the backscatter from these objects. The closed-form solutions described by Chen and Ling [1] model the EM backscattering based on the geometry and dimensions of objects, where simple geometric shapes are modelled. Chen, Lin and Pala [2] use the modulation features in Doppler spectra to estimate useful information about an object under test since the geometry, dimension, and rotation rate of the object are responsible for the characteristics in the spectrum. They describe the modelling of backscatter from various objects, including a rotating spinning top, and show the Doppler and time characteristics associated with them.

Specific to helicopter modelling, Whitrow and Cowley [3] describe the backscatter from a rotating plate used to simulate helicopter rotor blades. This investigation describes a closed-form solution for a rotating blade and relates the physical characteristics of the plate to features found in the time-domain data and Doppler spectrum.

Also, relevant to helicopter modelling, micro-Doppler effects such as mechanical vibrations and slow rotations, specific to the helicopter body, also contribute to the overall Doppler spectrum. Chen, Li et al [4] describe the micro-motion effects associated with these types of physical phenomenon and simulate the backscatter induced by targets that undergo these effects.

More numerically based modelling as seen in the research by Schneider [5] and Fliss [6] requires a greater level of detail in the modelling and hence greater processing cost. Schneider used an autoregressive process to model the frequency and amplitude modulation of the incident radar wave on a rotating object. Similarly, Fliss considered a point scatterer model to generate a Doppler modulated signal and later extended this model to a line scatterer model to simulate a helicopter rotor blade. Both these models assume the reflectivity is uniform along the blade giving rise to 'sinc' type responses in the time domain.

In this work, we report on new simple and useful analytical solutions that have not been reported in the open literature, extend the linear wire model to include non-uniform reflectivity along the wire, which may be used to model features such as varying cross-sectional area or material composition along a blade. Nuts, bolts, and corner reflector-like components of different sizes are modelled as vibrating point scatterers of various reflectivity coefficients.

For the standard simulation where the dominant scatterers are the rotor blades, rotor hub and helicopter body, the closed-form solutions achieve a reasonably accurate approximation to a radar return, and it is these models that are investigated in the most detail with the intention to combine them to model a backscatter signal from a complete heli-

copter. The short-time Fourier transform (STFT) analysis of the helicopter return signal, similar to those found in [7], will be used to analyse the features in the return specific to particular component objects.

The report is structured as follows. Section 2 describes in detail the closed-form solutions for a rotating wire, plate and rods in various orientations, including the vibrating effects from the helicopter body. Section 3 briefly discusses issues with numerical modelling, while Section 4 discusses results, in the form of time and frequency responses of the various configurations of a model helicopter. It also includes an interesting comparison with results from real helicopter data.

2 Exact Analytical Models

In the following, we set up the notation and briefly review the general (and well-known) analytical model of the return signal from a point target.

The transmitted radar signal can be modelled as a complex sinusoid with a variable amplitude:

$$s_T(t) = A(t)\exp\{-i(2\pi f_0 t + \phi_0)\}, \tag{1}$$

where f_0 is the (base) frequency of the transmitted signal, ϕ_0 is an arbitrary phase term, and $A(t)$ is the transmit amplitude profile.

For a point target which behaves like an impulse function to the impinging signal, the received signal can be written as [1] [2]

$$s_R(t) = \sigma A\left(t - 2\frac{r(t)}{c}\right)\exp\left\{-i\left[2\pi f_0\left(t - 2\frac{r(t)}{c}\right) + \phi_0\right]\right\}, \tag{2}$$

where σ is the reflectivity coefficient of the point target, $r(t)$ is the target range, and c is the speed of light. If the point target is a part of a larger object with 'centre' at range r_0, then one can rewrite

$$r(t) = r_0 + r_1(t),$$

such that $r_0 = v_0 t$ (say) captures the Doppler effect of the centre of the target, while $r_1(t)$ describes rotational effects of the point scatterer:

$$s_R(t) = \sigma A\left(t - 2\frac{r(t)}{c}\right)\exp\left\{-i\left[2\pi\left(f_0 - \frac{2v_0}{\lambda}\right)t - 4\pi\frac{r_1(t)}{\lambda} + \phi_0\right]\right\}, \tag{3}$$

where λ is the wavelength of the radar.

There are a number of valid assumptions that can help simplify the above expression a little further.

- Assuming that receiver blanking is not a problem, the amplitude profile $A(t)$ can be ignored;
- The usual frequency down conversion in the radar hardware and the shifting to zero of the body Doppler line at $2v_0/\lambda$ in the baseline processing means that the first term in (3) can be ignored. ϕ_0 is only a constant term and can also be ignored;

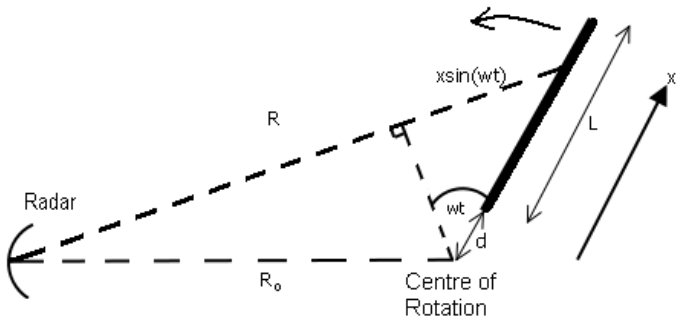

Figure 1: *Geometry of a rotating wire*

then what remains of the micro-Doppler signal of the rotating point-scatterer can be written simply as

$$s_R(t) = \sigma \exp\{i\phi(t)\} = \sigma \exp\{i\frac{4\pi}{\lambda} r_1(t)\}. \tag{4}$$

From here onward, we will re-write $r_1(t)$ as $r(t)$ for brevity.

For a single rotating point scatterer, the received signal model is derived simply and exactly from (4):

$$s_R(t) = \sigma \exp\{i\frac{4\pi}{\lambda} R\sin(\theta)\}, \tag{5}$$

where R is the radius and θ is the instantaneous angle. As will be seen later, the appearance of the $\sin(\theta)$ as a factor in the phase term is quite characteristic of rotating targets in general.

2.1 Rotor Blade Representation

This section presents simple analytical models for the rotor blade: as a one-dimensional rotating wire, or as a two-dimensional rectangular plate.

2.1.1 Blade as a Straight Wire

Here, a rotor blade is modelled as a radially oriented straight wire of length L, which can be theoretically represented as a continuous one-dimensional collection of point targets, as depicted in Figure 1. As such, it is a natural extension of the point target model described above.

Let x denote the position coordinate along the wire and ω the angular speed, then $r(t) = x\sin(\omega t)$, and Equation 4 becomes

$$s_R(t) = \sigma \exp\{ibx\sin(\omega t)\} \tag{6}$$

where $b = 4\pi/\lambda$, a constant. Therefore, for a wire of length L that is at a minimum distance d from the axis of rotation, the total signal due to the wire is

$$s_R(t) = \int_d^{d+L} \sigma \exp\{ibx\sin(\omega t)\}\, dx, \tag{7}$$

which leads to a convenient exact analytical result of

$$s_R(t) = \sigma L \exp\left\{ib(d + \frac{L}{2})\sin(\omega t)\right\} \text{ sinc}\left\{b\frac{L}{2}\sin(\omega t)\right\}, \tag{8}$$

where the 'sinc' term[1] describes the shape or amplitude modulation in time of the signal. Note that the periodic $\sin(\omega t)$ function appears as an argument of the amplitude sinc function that simulates the characteristic 'blade flashes' of the helicopter return signals.

Equation 8 gives the return signal due to only one wire. The total signal from N such wires, uniformly separated in angle, as in a typical helicopter rotor, can be computed by taking into account the initial angle of the k^{th} wire, $\theta_k = \theta_0 + 2\pi k/N$. Thus, the $\sin(\omega t)$ term only needs to be replaced by $\sin(\omega t + k2\pi/N)$, and the total return signal can be written as

$$s_R(t) = \sum_{k=0}^{N-1} \sigma_k L \exp\left\{ib(d + \frac{L}{2})\sin(\omega t + \frac{k2\pi}{N})\right\} \text{ sinc}\left\{b\frac{L}{2}\sin(\omega t + \frac{k2\pi}{N})\right\}. \tag{9}$$

An Example

Suppose two oppositely and radially oriented wires are illuminated by a pulse Doppler radar, each with geometry illustrated in Figure 1, wire length of 6 m, distance between the inner tip and center of rotation of 0.5 m, rotation speed of 300 RPM, a pulse repetition frequency (PRF) of 40 kHz and $f_0 = 10$ GHz. Then the simulated signal based on (9) are shown in Figure 2.

Figure 2(a) is the generated time domain samples exhibiting the 'blade flashes' characteristic of backscatter signals from helicopters, at 0.1 s intervals. The flashes result when a blade is oriented perpendicular to the radar line-of-sight at which the RCS is maximum.

Figure 2(b) shows the spectrum of only one blade flash, exhibiting some important features. Firstly, the blade body at the perpendicular orientation produces a plateau region which extends from low frequencies to an edge corresponding to the 'tip Doppler', given by

$$\begin{aligned} f_{max} &= \frac{2\,\omega\,R}{\lambda} \\ &= \frac{2 \times 31.4 \times 6.5}{0.03} = 13.6 \text{ kHz} \end{aligned} \tag{10}$$

where $R = L + d$ is the radius of the wire. The spectrum also shows the low magnitude region around 0 Hz where no backscatter exists as the inner tip of the wire is offset from the centre of rotation by 0.5 m. Note that the radar reflectivity along the blade length is assumed constant. Secondly, spectral oscillations exist near the edge of the plateau making it difficult to determine precisely the tip Doppler. Thirdly, the relative magnitudes of the plateau in the negative and positive Doppler regions can be different, because of possible differences in reflectivity between the receding and advancing edges. For this example, we have used a smaller value for the reflectivity when the wire is approaching than when it is receding, which is consistent with observations in real data. Finally, the existence of a

[1] We use the definition sinc $x = \sin x/x$.

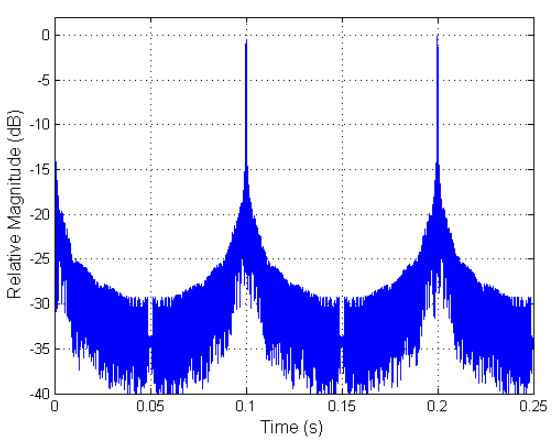

(a) Signal with several blade flashes in time domain

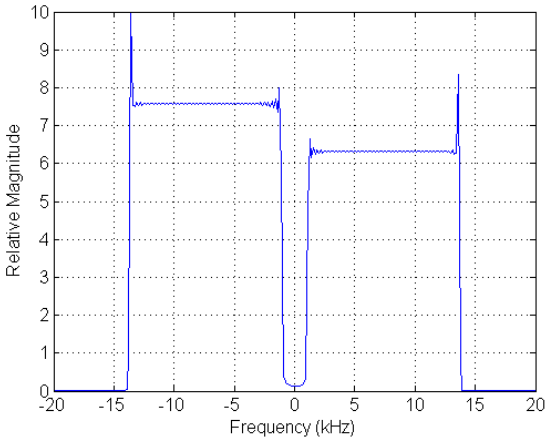

(b) Spectrum of one blade flash

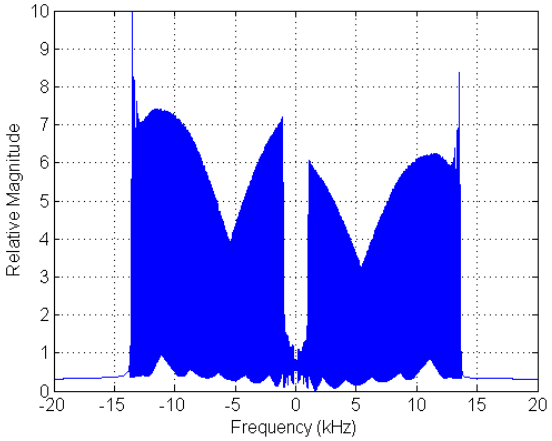

(c) Spectrum of the flashes in (a)

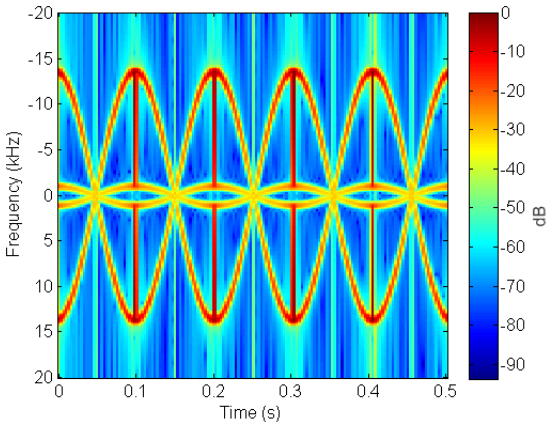

(d) Spectrogram of signal in (a)

Figure 2: *Time and frequency plots of a simulated signal for a two-wire rotor. Plots normalised to peak signal.*

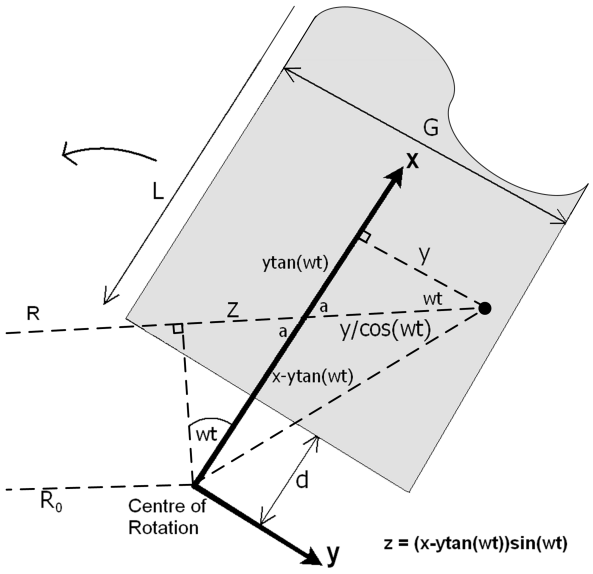

Figure 3: *Geometry of rotating flat plate*

two-sided spectrum (i.e. both positive and negative) indicates an even number of blades. If the number of blades is odd, then not more than one blade can be oriented perpendicular to the radar line-of-sight (LOS) at any one time giving a one-sided spectrum.

Figure 2(c) is the Doppler spectrum of several blade flashes shown in (a), showing a plateau modulated by the multiple flashes. Figure 2(d) is a time-frequency plot, called a spectrogram, which is a collection of contiguous short-time spectra, showing the evolution of the spectrum as the blades rotate. Flashes at 0.1 s intervals can be seen for both the receding and advancing wires, as discussed earlier. It can also be seen that the wire tips produce easily recognisable sinusoidal traces.

2.1.2 Blade as a Rectangular Flat Plate

Another model used to represent a rotor blade is the rectangular flat plate, with its surface in the (x, y) plane while the axis of rotation of the rotor is z, and the radar LOS may be at a small inclination angle of α with the (x, y) plane. Strictly speaking, this configuration is more relevant to a bistatic radar geometry than a monostatic radar, since a monostatic radar would receive most of its backscatter signal from surfaces around the plate edges, not so much from the interior part of the plate, and hence will not be validated against real data in the later sections of this work. Nevertheless, the theoretical merit of the model deserves a description here. It is also useful for obtaining another useful result for the 'horizontal rod' discussed in Section 2.2.2.

Let L and G respectively denote the length and width of the rectangular plate, while d is the distance from the inner edge to the axis of rotation, as depicted in Figure 3. The plate can be thought of as the limit of a two-dimensional array of point scatterers discussed earlier. For simplicity, we also assume that the inclination angle α is zero. Let x and y

denote the coordinates of a single point in the plate; R and R_0 denote the ranges to the single point and the center of rotation, then

$$R = R_0 + (x - y\tan(\omega t))\sin(\omega t) + \frac{y}{\cos(\omega t)}. \tag{11}$$

Using Equation 4 as the model for the single point scatterer, the return signal due to the whole plate is an integration over the entire rectangular plate:

$$s_R(t) = \int_d^{d+L}\int_{-G/2}^{G/2} \sigma \exp\left\{ib\left[(x - y\tan(\omega t))\sin(\omega t) + \frac{y}{\cos(\omega t)}\right]\right\} dydx, \tag{12}$$

where terms proportional to R_0 and not dependent on x, y or t have been removed for clarity. Evaluating the above integral leads to a close-form analytical result:

$$\begin{aligned} s_R(t) &= \sigma GL \exp\left\{(d + \frac{L}{2})ib\sin(\omega t)\right\} \times \\ &\quad \operatorname{sinc}\left[b\frac{L}{2}\sin(\omega t)\right] \operatorname{sinc}\left\{b\frac{G}{2}\left[\frac{1}{\cos(\omega t)} - \tan(\omega t)\sin(\omega t)\right]\right\}. \end{aligned} \tag{13}$$

For N rotating plates, the composite signal can be found by the linear sum

$$s_R(t) = \sum_{k=0}^{N-1} s_{R_k}, \tag{14}$$

in which ωt is replaced by $\omega t + k2\pi/N$.

An Example

A rotor with three flat plates is illuminated by a pulse Doppler radar, each with a blade length of 6 m, width of 0.5 m, offset from the centre of rotation of 0.5 m, angular speed of 300 RPM; and the radar uses a PRF of 40 kHz and a carrier frequency f_0 of 10 GHz. The resulting backscatter signal is shown in Figure 4.

Figure 4(a) is the time-domain signal showing the blade flashes at 0.033 s intervals, which occur when any one of the three plates are oriented perpendicular to the radar LOS. The other sub-figures illustrate features similar to that of the straight wire model discussed earlier, except that in this case, the spectrum for a single blade flash is single-sided, as the number of blades is odd[2].

2.1.3 Blade as a Rectangular Flat Plate - The Whitrow-Cowley Model

The Whitrow-Cowley model was developed at DSTO in the 1980s [3]. Like the model discussed in the preceding section, it too models a blade as a rectangular flat plate, except that here the plane of the plate contains the axis of rotation, as depicted in Figure 5.

[2]The distinction between double-sided and single-sided spectra is only meaningful for a single blade flash. For multiple flashes, it is necessarily always double-sided.

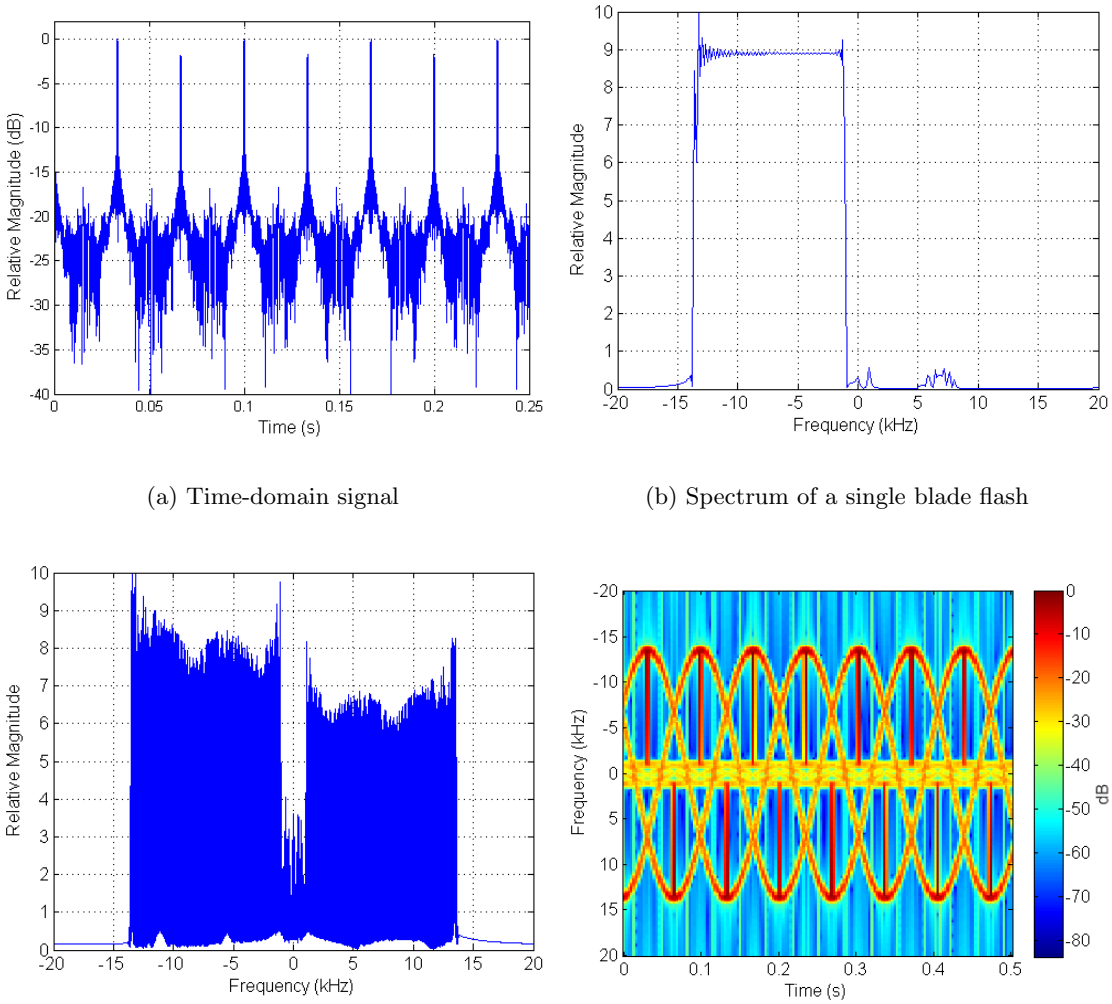

(a) Time-domain signal

(b) Spectrum of a single blade flash

(c) Spectrum of the time signal in (a)

(d) Spectrogram of the signal in (a)

Figure 4: *Time and frequency plots of a simulated signal for a three-plate rotor. Plots normalised to peak signal.*

This model has more relevance for the backscattering of the monostatic radar as the plate orientation means a significant portion of the scattered RF energy can be expected to be received by the radar, in typical radar-helicopter engagement scenarios.

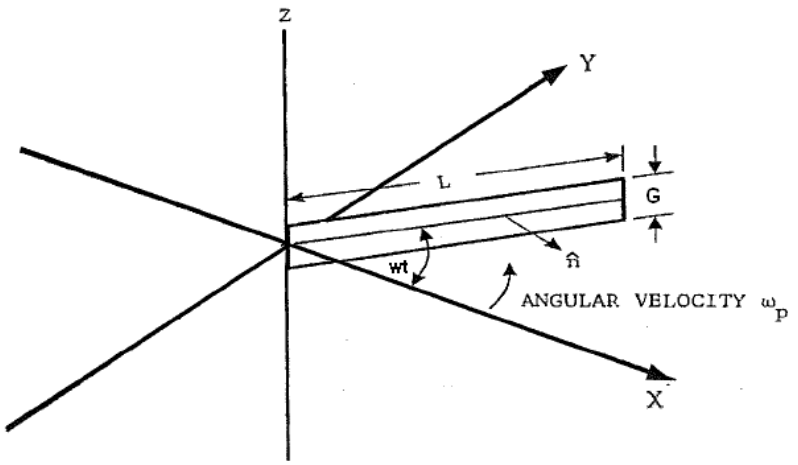

Figure 5: *Geometry of rectangular flat plate in the Whitrow-Cowley model*

Fortunately, the solution for $s_R(t)$ to this case is also available in closed form, with details of the derivation found in [3]. In the current notation, the solution is

$$s_R(t) = V_0 \exp\left\{-i\frac{2\pi}{\lambda}L\cos(\beta)\sin(\omega t)\right\} \operatorname{sinc}\left\{\frac{2\pi}{\lambda}L\cos(\beta)\sin(\omega t)\right\} |\cos(\omega t)|, \qquad (15)$$

where V_0 is a constant that absorbs the length and width of the plate and β is the inclination angle. Like the other models, the substitution $\omega t \rightarrow \omega t + k2\pi/N$ in the solution and the summation for $k = 0$ to $N - 1$ would give the total return signal for the general case of an N-blade rotor[3].

2.2 Rotor Hub Representation

In our model, a rotor hub is represented by an ensemble of rods and scattering centres in various orientations and relative positions. The idea was motivated by the fact that structural components of a real helicopter rotor hub are usually control rods, nuts and bolts, and objects that resemble corner reflectors. For even more 'serious simplicity', a rod is modelled as a straight wire segment and a scattering centre as a point scatterer [1]. How such an ensemble should be put together will be discussed for specific examples in the following sections.

2.2.1 Rods

Let us now consider the case of a rod of length L that is oriented at some angle ϕ to, and coplanar with, the axis of rotation, as depicted in Figure 6. (When ϕ is zero, the case

[3]Unlike other blade models derived, the Whitrow-Cowley model does not include a term for the distance from the axis of rotation to the start of the blade, d. It assumes that $d = 0$.

reduces to a radial wire considered in Section 2.1.1). For simplicity of analysis, we assume the midpoint of the rod and the radar all lie in the (x, y) plane.

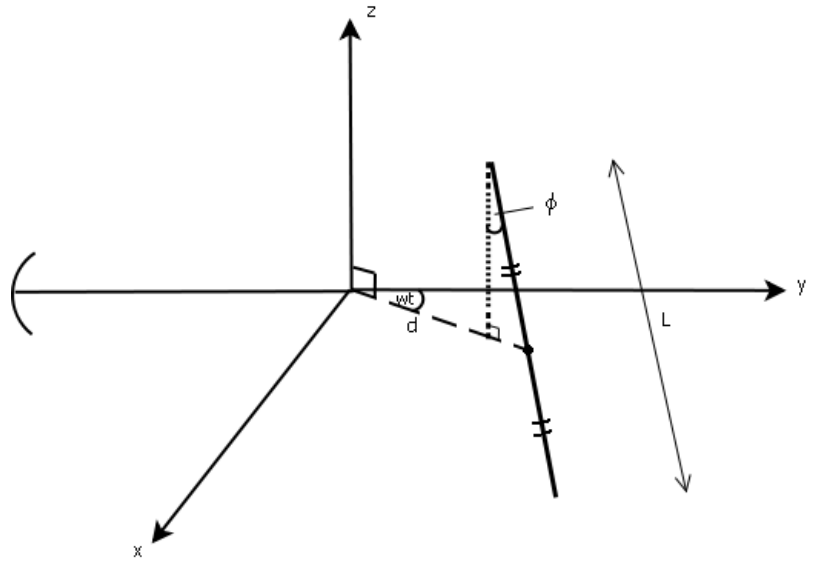

Figure 6: *Geometry of a rod as a component of a rotor hub*

Let x to be the distance coordinate along the rod relative to the midpoint and d to be the distance from the centre of rotation to the midpoint; it can be shown that the horizontal distance from the centre of rotation to the point at position x along the rod is $d + x\sin(\phi)$. Refer to Figure 7. For $R_0 \gg d$, one can approximate the range of a point on the rod as

$$R = R_0 + \sin(\omega t)(d + x\sin\phi). \tag{16}$$

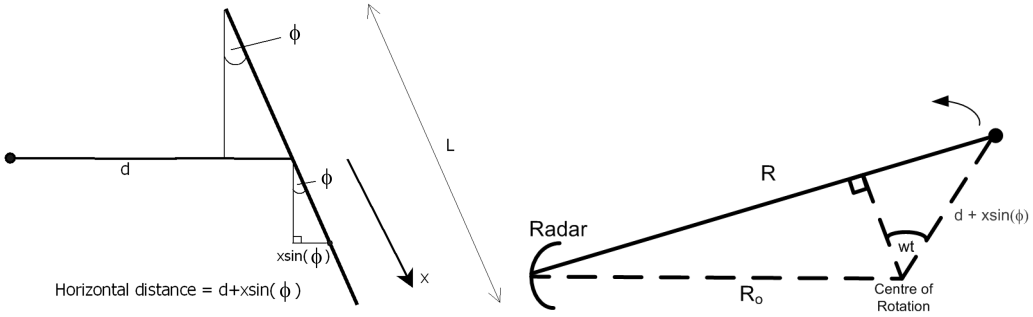

(a) Geometry of System from Centre of Rotation

(b) View from Above

Figure 7: *Geometry of a rod*

Using (4) for an individual point, the backscattered signal from the rod is an integration given by

$$s_R(t) = \int_{-L/2}^{L/2} \sigma \exp\left\{ i\frac{4\pi}{\lambda}[R_0 + \sin(\omega t)(d + x\sin\phi)] \right\} dx, \tag{17}$$

which is found to be expressible in the simple close form of

$$s_R(t) = \sigma L \exp\left\{i\frac{4\pi}{\lambda} d \sin(\omega t)\right\} \operatorname{sinc}\left\{\frac{2\pi}{\lambda} L \sin(\phi)\sin(\omega t)\right\}. \tag{18}$$

Taking into account the angle of elevation/depression from the radar source to the target and using the substitution

$$b \equiv \frac{4\pi}{\lambda}\cos\beta \tag{19}$$

the backscattered signal is

$$s_R(t) = \sigma L \exp\{ibd\sin(\omega t)\} \operatorname{sinc}\left\{b\frac{L}{2}\sin(\phi)\sin(\omega t)\right\}. \tag{20}$$

An Example

Two rotating rods, symmetric around the centre of rotation, are illuminated by a pulse Doppler radar with a PRF of 40 kHz and carrier frequency of 10 GHz. The rods are 4 m long, inclined 18° to the axis of rotation, offset from the centre of rotation by 1.4 m and the angular speed is 300 RPM. The resulted signal is shown in Figure 8. Note that flashes still occur, similar to the case for the blades. The two clearly visible sinusoidal traces in the spectrogram correspond to the tips of the rods.

2.2.2 Horizontal Rod

Instead of being co-planar with the axis of rotation, a rod can also be oriented perpendicular to both the axis of rotation and the radial direction, i.e. it lies tangential to the circular motion of its mid-point, as depicted in Figure 9.

If d corresponds to the distance from the centre of rotation to the midpoint, assuming that this line connecting midpoint to centre of rotation is also perpendicular to the rod, then the radar range of any point of the rod can be approximated as

$$R = R_0 + [d - x\tan(\omega t)]\sin(\omega t) + \frac{x}{\cos(\omega t)} \tag{21}$$

where x is the position coordinate along the rod relative to the midpoint. The simple geometry facilitates an analytically convenient integral to be calculated for the return signal as

$$\begin{aligned} s_R(t) &= \int_{-L/2}^{L/2} \sigma \exp\left\{ib\left[R_0 + (d - x\tan(\omega t))\sin(\omega t) + \frac{x}{\cos(\omega t)}\right]\right\} dx \\ &= \sigma L \exp\{ibd\sin(\omega t)\} \operatorname{sinc}\left\{b\frac{L}{2}\left[\frac{1}{\cos(\omega t)} - \tan(\omega t)\sin(\omega t)\right]\right\}. \end{aligned} \tag{22}$$

where L is the length of the rod.

The above result may also be achieved as a limiting case of the rectangular flat plate solution (13) considered in Section 2.1.2, by letting the length dimension approach zero.

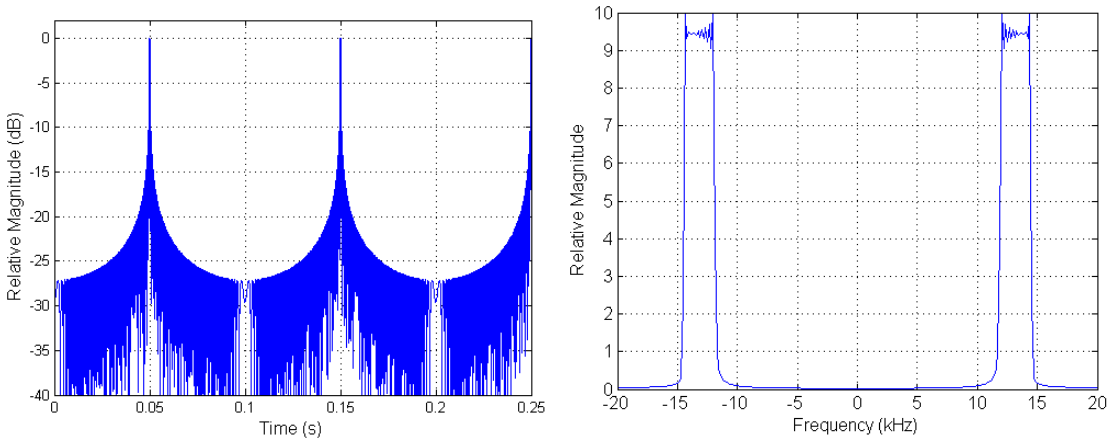

(a) Time-domain signal of several flashes

(b) Spectrum of one flash

(c) Spectrum of the several flashes in (a)

(d) Spectrogram of the flashes in (a)

Figure 8: *Signal plots of two rotating rods, inclination of* 18°. *Plots normalised to peak signal.*

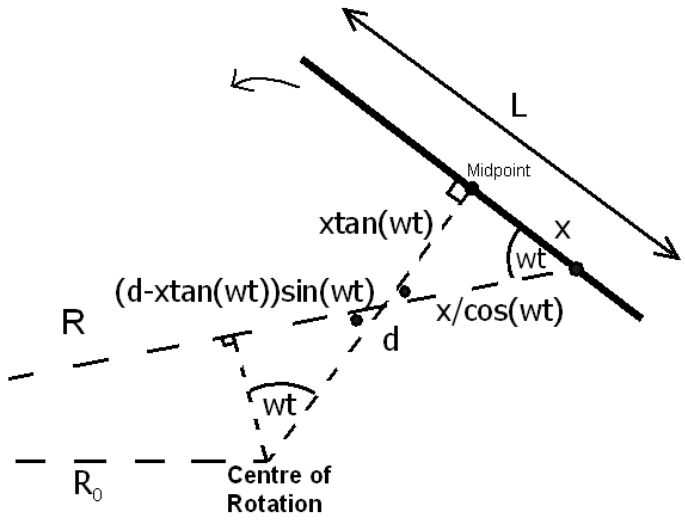

Figure 9: *Geometry of horizontal rod system*

An Example

A rotating horizontal rod 4 m long, at a radius of 1.4 m and rotating with an angular speed of 300 RPM is illuminated by a pulse Doppler radar with a PRF of 40 kHz and carrier frequency of 10 GHz. The signal generated by the above analytical result is shown in Figure 10. Note the distinctive spectral region around zero, and the two sinusoidal traces of the rod tips following each other, as opposed to the previously discussed examples.

2.3 Helicopter Body Representation

The signal component backscattered by the helicopter body is statistically the strongest component in the signal, and hence should not be ignored in a simulation. High-fidelity simulation of this component would require numerically intensive methods such as the finite element method. In our simple context, we model it as a collection of vibrating point scatterers, with the vibration frequency typically in the audio range. How many such point scatterers should be used, or what type of random variation on the signal amplitude to simulate signal scintillation are questions to be answered later based on trial and error experiments and comparison with real data.

For the sake of completeness and reference convenience, we summarise in this section an analytical solution for a single vibrating point scatterer as has been reported by Chen and Li in [4].

Referring to the coordinate system for the point scatterer in Figure 11, in which the centre of the scatterer's vibration is given by the spherical coordinates (R_0, α, β), where α and β are the azimuth and elevation angles respectively. Let the vibration rate and amplitude of the point scatterer be ω_v and D_A respectively. One can then define a new coordinate system at this vibration centre such that the point scatterer is at position (D_t, α_p, β_p), where α_p and β_p are the vibration azimuth and elevation angles respectively,

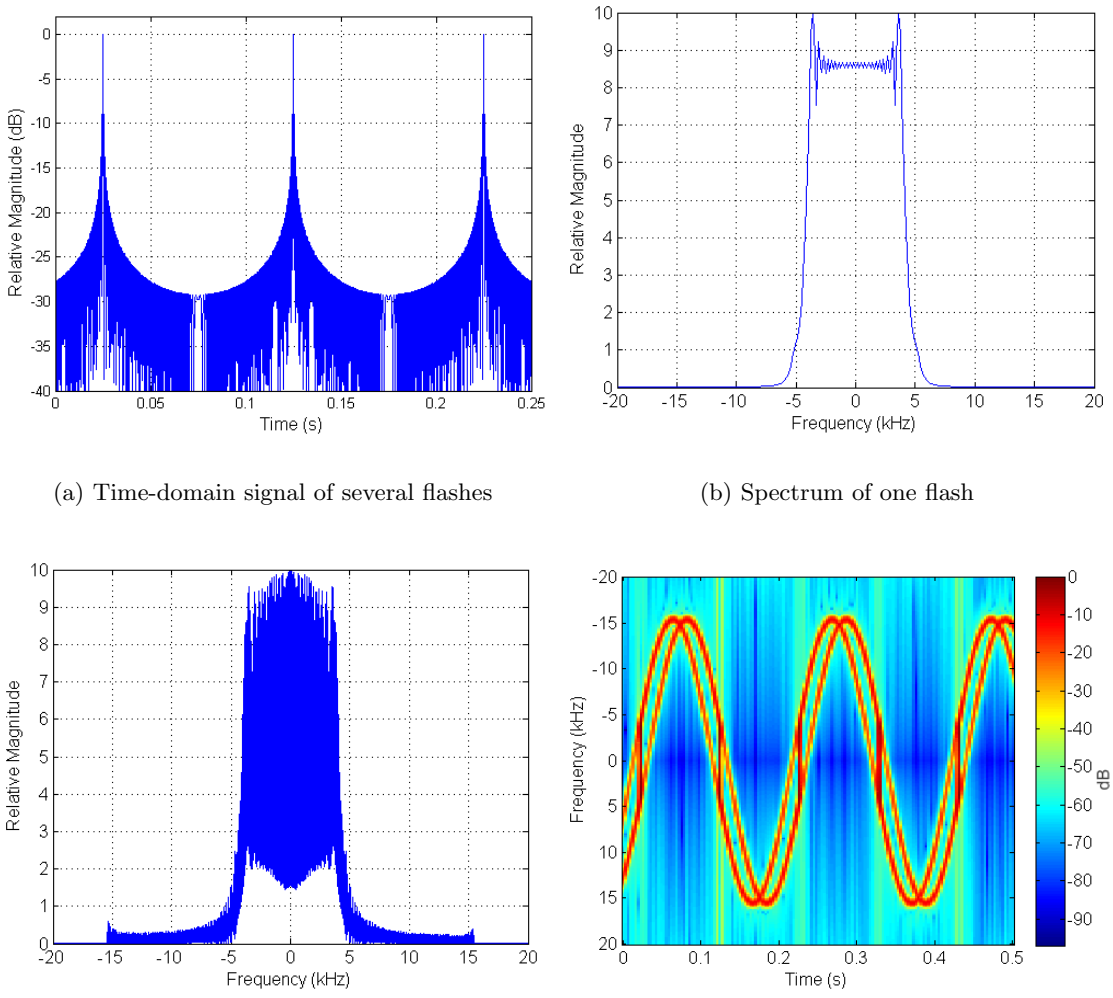

(a) Time-domain signal of several flashes

(b) Spectrum of one flash

(c) Spectrum of the several flashes in (a)

(d) Spectrogram of the flashes in (a)

Figure 10: *Plots of the signal from a rotating horizontal rod. Plots normalised to peak signal.*

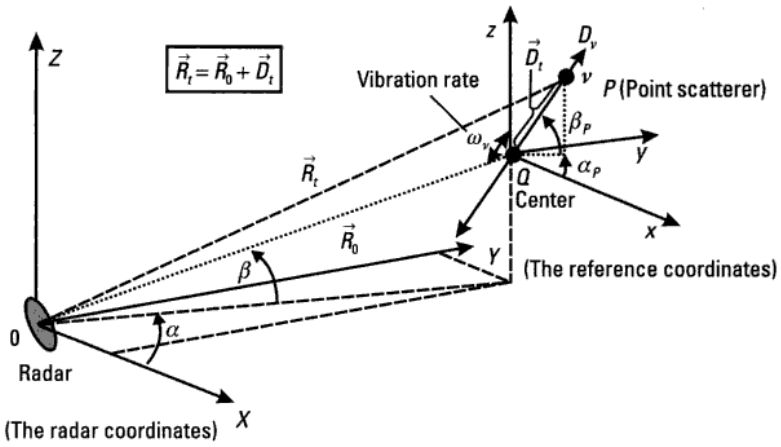

Figure 11: *Geometry of a vibrating point scatterer (adapted from Chen and Li [4])*

and D_t represents the distance from the vibrating centre to the point and can be expressed as $D_t = D_A \sin(\omega_v t)$.

The distance from the radar source to the vibrating scatterer is given by the vector sum of the distance to the vibration centre and the distance from the vibration centre to the point scatterer,

$$\overrightarrow{R_t} = \overrightarrow{R_0} + \overrightarrow{D_t}. \tag{23}$$

Making the assumption that $R_0 \gg D_A$, according to Chen & Ling [1], one can express the distance from the radar source to the scatterer as

$$R = \mid \overrightarrow{R_t} \mid \approx R_0 + D_A \sin(\omega_v t)\,[\cos(\beta)\cos(\beta_p)\cos(\alpha - \alpha_p) + \sin(\beta)\sin(\beta_p)]. \tag{24}$$

Thus, using Equation 4 as the model for the radar return signal, the return due to the vibrating point scatterer is

$$s_R(t) = \sigma \exp\{i\frac{4\pi}{\lambda}[R_0 + D_A \sin(\omega_v t)(\cos(\beta)\cos(\beta_p)\cos(\alpha - \alpha_p) + \sin(\beta)\sin(\beta_p))]\}. \tag{25}$$

We may also use the vibrational frequency, f_v, by making the substitution $\omega_v \rightarrow 2\pi f_v$, where f_v is the vibrational frequency of the point scatterer.

2.4 Some Special Closed-Form Solutions

As a useful theoretical adventure, we explored the existence of close-form solutions to the integral in Equation (7) for the cases where the reflectivity coefficient $\sigma(x)$ is not a constant but some simple function of x. It turns out that the integral in (7) is amenable to simple closed solutions when $\sigma(x)$ is either a linear, an exponential, or a sinusoidal function. In most other cases, the integral can only be evaluated numerically.

The closed form solutions are summarised as follows. For $\sigma(x) = ax$,

$$s_R(t) = a\,L\,e^{i(d+L/2)g(t)}\left[\frac{\exp\{iLg(t)/2\} - \mathrm{sinc}\{L\,g(t)/2\}}{ig(t)} + d\,\mathrm{sinc}\left\{\frac{L}{2}\,g(t)\right\}\right], \tag{26}$$

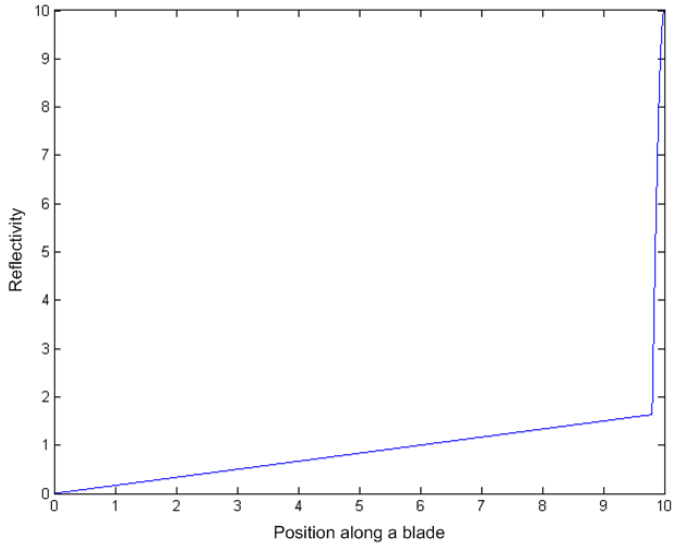

Figure 12: *Example of a linear reflectivity profile with cosine tip term, $\varepsilon = 0.2$.*

for a radially oriented rotating wire, or

$$s_R(t) = a\,L\,e^{id\,g(t)}\left\{\frac{L}{2}\,\mathrm{sinc}\left[\frac{L}{2}\sin(\phi)g(t)\right] - \frac{\mathrm{sinc}(\frac{L}{2}\sin(\phi)g(t))}{i\sin(\phi)g(t)}\right\}, \tag{27}$$

for rod. Here, $g(t) = b\sin(\omega t)$. Other notations are explained in previous sections.

For $\sigma(x) = ae^{-mx}$,

$$s_R(t) = \frac{a}{ig(t) - m}e^{d(ig(t)-m)}(e^{L(ig(t)-m)} - 1), \tag{28}$$

for a radially oriented rotating wire, or

$$s_R(t) = a\,Le^{id\,g(t)}\,\mathrm{sinc}\{\frac{L}{2}(\sin(\phi)g(t) + im)\}, \tag{29}$$

for rod.

For sinusoidal functions, it is most practically relevant to use them to model the tip of a blade, which is where significant specular reflection of the EM waves can occur, relative to the body of a blade. A hypothetical profile for $\sigma(x)$ involving a linear segment followed by a steep cosine function at the tip is shown in Figure 12. For the tip part, suppose

$$\sigma(x) = a\cos(nx - n(d + L)) \text{ for } d + L - \varepsilon \le x \le d + L,$$

then

$$\begin{aligned} s_R(t) &= \int_{d+L-\varepsilon}^{d+L} ae^{ixg(t)}\cos(nx - n(d + L))dx, \\ &= \frac{ae^{i(L+d)g(t)}}{g(t)^2 - n^2}[-ig(t) - e^{-i\varepsilon g(t)}(n\sin(n\varepsilon) - ig(t)\cos(n\varepsilon))]. \end{aligned} \tag{30}$$

3 Numerical Considerations

As has been mentioned earlier, without resorting to numerically intensive approaches, as mentioned in [5] and [6], we are attempting to simulate a reasonably realistic backscatter signal of a helicopter target based on simple theoretical models. Although we have a two dimensional solution for the rectangular plate model, all the numerical computation in this work involves at most one dimensional integration; in other words, the numerical computation is linear, to minimise the computational cost. Nevertheless, many numerical issues involved need still be considered, and are the subject of discussion in this section.

Numerical consideration for each scattering component is necessary in the following possible situations:

- Structural components along a blade, or within the rotor hub, behave as discrete scattering centres which are best modelled as point-scatterers with differing RCS values. Possible examples include nuts and bolts, or small edges and crevices.
- Because of the peculiar shape or material composition, a blade or a rod is best modelled as a straight wire but with a variable reflectivity function $\sigma(x)$ that is not amenable to analytical solutions.
- Within the current limited context, the body return component will be modelled as a collection of vibrating point scatterers with an associated scintillation effect.

The rotating point scatterer can be a satisfactory, and yet simple model for a blade tip if used with an RCS value that is a function of the angle of rotation, or for any discrete scattering center along a blade or inside a hub.

For a single rotating point scatterer, and within the micro-Doppler context, it should be noted that it is not necessary to model its Doppler frequency f_d separately, because the product $f_d t$ is equivalent to $2\,r(t)/\lambda$. Only the phase due to its instantaneous range needs to be modelled.

The phase due to the instantaneous range of the point scatterer is [6]

$$\phi(t) = \frac{-i4\pi}{\lambda} r(t) \approx \frac{-i4\pi}{\lambda} R\,\sin(\theta), \tag{31}$$

relative to the centre of rotation. The total phase function of the rotating point scatterer is $\phi(t)$, assuming the Doppler component of the rotation centre has been filtered out.

For multiple point scatterers, such as those on multiple blades or multiple positions in a hub, both the relative angular and radial positions, for each scatterer, need to be accounted for. For angular positions in particular, the angle for the m^{th} scatterer is

$$\theta_m = \frac{2\pi m}{M} + 2\pi\omega t \tag{32}$$

where m is the m^{th} scatterer under consideration and M is the total number of scatterers.

The total backscatter signal is the linear sum

$$s(t) = \sum_{m=1}^{M} A_m \exp\{\phi_m(t)\}, \tag{33}$$

where A_m are the amplitudes of the scattered signals, which may be varying with time and depend on relative position. The sum in (33) can also be used to approximate the integral for a straight wire model when $\sigma(x,t)$ is an arbitrary function.

4 Results

In this section a simulated radar return from models is generated that represents three hypothetical helicopters (a simple, moderately complex and complex case) and investigates the elements of the signal in the time and frequency domains. Also, an additional simulated radar return is generated from a model that represents an actual helicopter, whose real radar data is available for comparison.

This section describes the models used, the process involved in emulating the real helicopter rotor, and an analysis of the radar returns using time and frequency domain techniques.

4.1 Hypothetical Helicopter Modelling

For the hypothetical cases, a pulse Doppler radar, with a carrier frequency of 10 GHz and PRF of 40 kHz, illuminates a stationary helicopter whose rotor is rotating with a angular speed of 300 RPM.

4.1.1 A Simple Rotor Configuration

The geometry of the simple hypothetical rotor is shown in Figure 13(a). This rotor model consists of two rotating wires representing rotor blades, each of length 5 m, offset from the centre of rotation by 1 m and whose reflectivity of the receding wire is 1.5 times larger than the advancing wire to simulate the difference in blade RCS. Also, two almost vertically oriented rods, as defined in Section 2.2.1, representing a specific feature in the rotor hub are included. The rods are 1.0 m long and are offset from the centre of rotation by 1.0 m and at 20° to the axis of rotation. The body of the helicopter is not modelled.

Figure 13(b) is the time-domain signal showing the blade flashes at 0.1 s intervals corresponding to the time at which the rotor wires are perpendicular (or broadside) to the radar LOS. Similarly, the flashes that occurs at the time of 0.05 s, correspond to the flashes from the vertical rods and also occur at 0.1 s intervals. The magnitude of these flashes are lower in magnitude due to the shorter rod lengths when compared to the rotor blades. Note, the slight inclination of the rods with the axis of rotation produces forward scattering for off-broadside angles, giving small returns for these angles.

Figure 13(c) shows spectra of one flash generated by the wire and rod when they are perpendicular to the radar LOS. The spectrum from the blade flash is typical for this type of object, which is discussed in Section 2.1.1. The spectrum exhibits the typical features such as the blade body plateau which extends from the blade's inner tip (offset from the centre of rotation) to the blade's outer tip and difference in plateau magnitudes in the

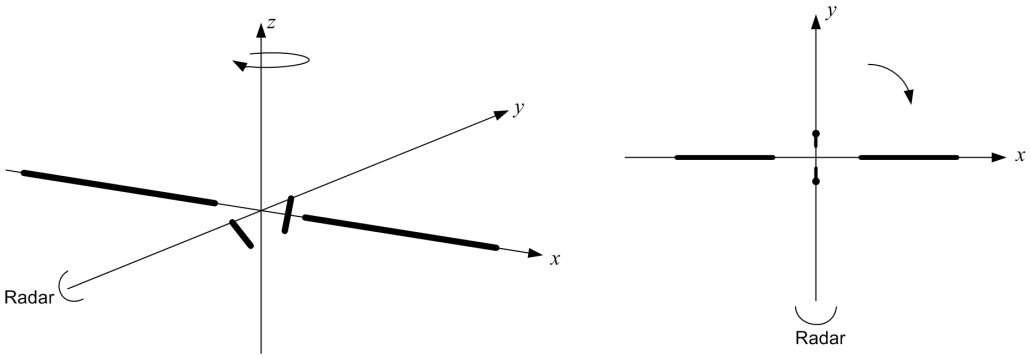

(a) An orthographic (left) and planar view(right) depicting the geometry of a simple hypothetical helicopter rotor consisting of two rotating wires and two vertical rods.

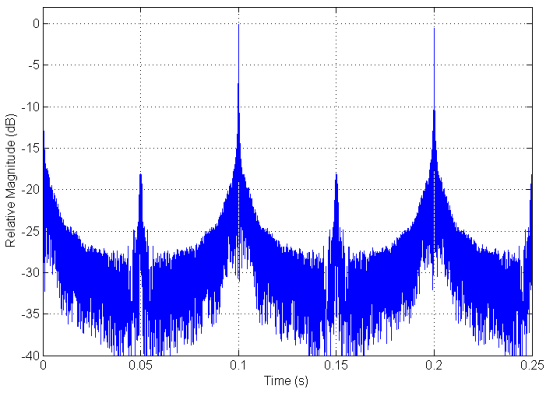

(b) Time-domain signal

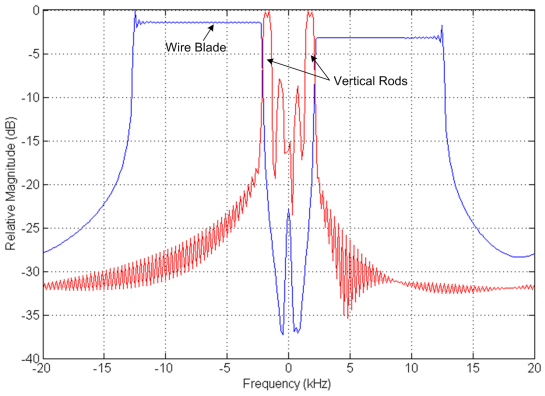

(c) Blade and vertical rod flash spectra

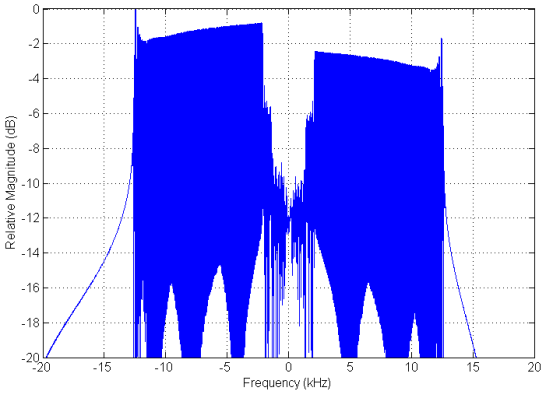

(d) Frequency-domain signal

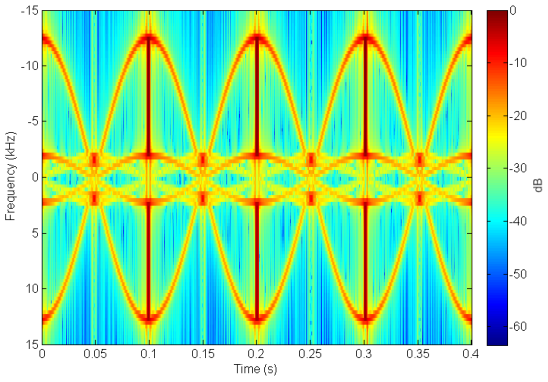

(e) Spectrogram

Figure 13: *Time and frequency plots of a simulated signal from the simple hypothetical helicopter illuminated by a 10 GHz radar with a PRF of 40 kHz. Plots normalised to peak signal.*

negative and positive Doppler regions. The spectrum from the rod flash is also very typical for this orientation and it's Doppler extent is relative to the the rod's physical size.

Figure 13(d) is the spectrum of multiple flashes and Figure 13(e) is the spectrogram showing the evolution of the spectrum during rotation. This is a combination of the wire and rod spectrograms and partially validates the modelling process described here. The blade flashes occur at 0.1 s intervals with the tips giving the typical sinusoidal trace and the rods providing the intermediate flashes.

4.1.2 A Moderately Complex Helicopter Configuration

The geometry of a moderately complex hypothetical helicopter is shown in Figure 14(a). This helicopter model consists of two rotating wires similar to the simple case but with the reflectivity of the blade varying along the blade length. This variability is numerically calculated for this case. Also, a vertically oriented rod and a horizontal rod represent two specific features in the rotor hub. The rod is 1.0 m long and offset from the center of rotation by 0.5 m and at 15° to the axis of rotation. The horizontal rod is 1 m long and offset from the centre of rotation by 0.8 m.

In this case, the body of the helicopter is modelled as a vibrating point scatterer located 1 m below the rotor's centre of rotation. This scatterer, as defined in Section 2.3, is vibrating in the *y-plane* giving the maximum displacement with respect to the radar and as such the vibrational azimuth and elevation is zero. The vibration amplitude and frequency is 0.05 and 100 Hz respectively. Note, the vibrational amplitude and frequency values were chosen such that the vibrating scatterer is easily identifiable in the time and frequency analysis.

Figure 14(b) is the time-domain signal showing flashes from the blade body and vertical rod. Again, the blade flashes occur at 0.1 s intervals with the vertical rod flashes occurring midway between blade flashes at the same interval. The horizontal rod will give a flash when it's orientation is perpendicular to the radar LOS, occurring at the same time as the blade flashes. The relatively smaller horizontal rod, when compared to the blade length, gives a smaller return and cannot be seen in this domain. Also visible in this plot is the small contribution of the vibrating scatterer during the capture time.

Figure 14(c) shows the spectrum of one flash generated by the wire and horizontal rod when they are perpendicular to the radar LOS and superimposed on the same plot is the spectrum of one flash generated by the vertical rod. Again, the wire spectrum is typical of what has been seen previously except for the plateau where the varying blade reflectivity produces variablity in this region.

The horizontal rod produces a contribution in the low frequency region spanning ±1.5 kHz. The return from the single vertical rod produces a typical single-sided response since there is only one rotating rod. In this case the rod is moving away from the radar giving a negative Doppler.

Figure 14(d) and Figure 14(e) shows the frequency-domain signal and time-frequency plots respectively. Apart from exhibiting a typical return for the wire and rods as seen previously, the important feature seen here is the contribution from the vibrating scatterer which gives a low frequency oscillation. Although the amplitude and frequency of the

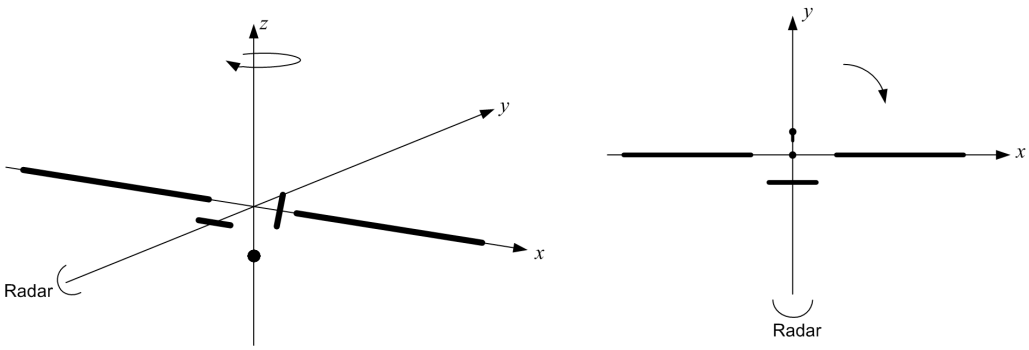

(a) An orthographic (left) and planar view (right) depicting the geometry of a complex hypothetical helicopter rotor consisting of two rotating wires, a vertical rod and a horizontally oriented rod.

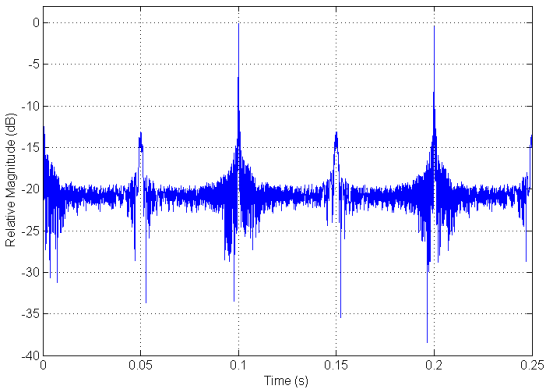

(b) Time-domain signal

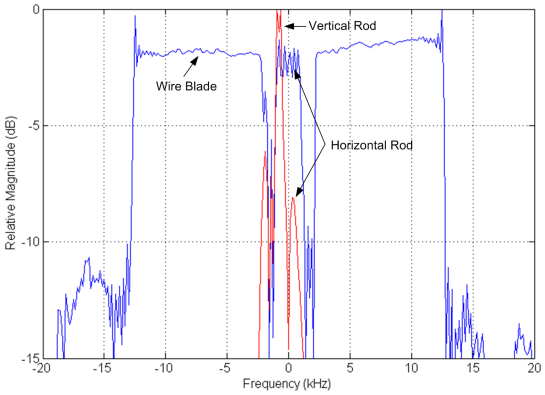

(c) Blade, vertical and horizontal rod flash spectra

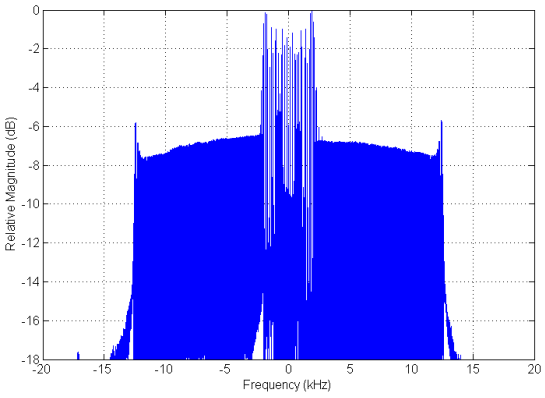

(d) Frequency-domain signal

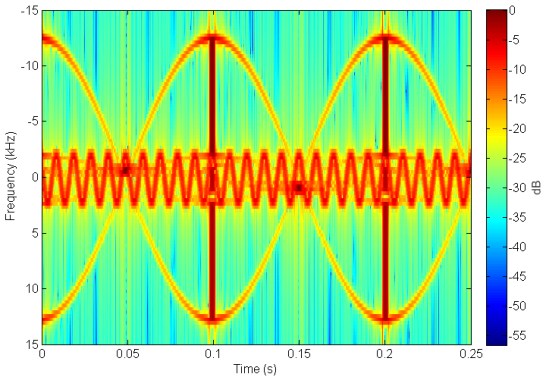

(e) Spectrogram

Figure 14: *Time and frequency plots of a simulated signal from the moderately complex hypothetical helicopter illuminated by a 10 GHz radar with a PRF of 40 kHz. Plots normalised to peak signal.*

vibration has been chosen to highlight this effect, the nature of the response is the critical observation and will aide in modelling a real helicopter and relating it to real data.

4.1.3 A Complex Helicopter Configuration

The geometry of a complex hypothetical helicopter is shown in Figure 15(a). This helicopter model consists of four rotating wires with parameters the same as the simple case, two vertically oriented rods and two horizontal rods. The rods are positioned 45° to the wire blades. The rods are 1 m long and offset from the centre of rotation by 1.4 m and at 20° to the axis of rotation. The horizontal rods are 1 m long and offset from the center of rotation by 1.7 m. Also, a vibrating point scatterer is located 1 m below the rotor's centre of rotation with a vibrational amplitude of 0.01 and vibrational frequency of 300 Hz.

Figure 15(b) is the time-domain signal showing flashes from the blade body and vertical rod. Note that the flash from the vertical rod and horizontal rod occurs every half rotation. Also visible in this plot is the small contribution of the vibrating scatterer during the capture time.

Figure 15(c) shows the spectrum of one flash generated by a wire when it is perpendicular to the radar LOS and superimposed on the same plot is the spectrum of one flash generated by the vertical rods and horizontal rods. Also, the vibrating scatterer contributes to the low frequency terms. Note that the wire blades produce a significant return when they are positioned at 45° with respect to the radar LOS. The time-frequency plot shown in Figure 15(e) shows this with the trace of adjacent blade tips overlapping at ±8 kHz, which is confirmed in Figure 15(c).

Figure 15(d) and Figure 15(e) shows the frequency-domain signal and time-frequency plots respectively. A typical return can be seen with the vertical rods and horizontal rods visible in each plot. The increase in vibrational frequency of the vibrating scatterer produces are more oscillatory response.

4.2 Comparison with Real Helicopter Data

Real radar data was measured using a pulse Doppler radar with carrier frequency 5.761 GHz and a PRF of 16.639 kHz. By inspection of the data the rotor rotation rate was estimated at 383 RPM. Using the objects discussed in this report, a composite model representing this actual helicopter is generated and a simulated radar signal is compared with real data.

The helicopter rotor and hub is a complex structure making a detailed representation impossible. The inclusion of noise and the actual radar environment cannot be modelled since these parameters are unknown. Only the main scattering centres are modelled and the comparison will be limited to these objects with more subtle effects in the real data ignored.

Figure 16 shows time-domain plots of the simulated and real data with various filtering techniques applied to highlight specific regions of interest. The blade returns are typically high frequency signals in the range 2 kHz to 8 kHz for this data set. By filtering out the

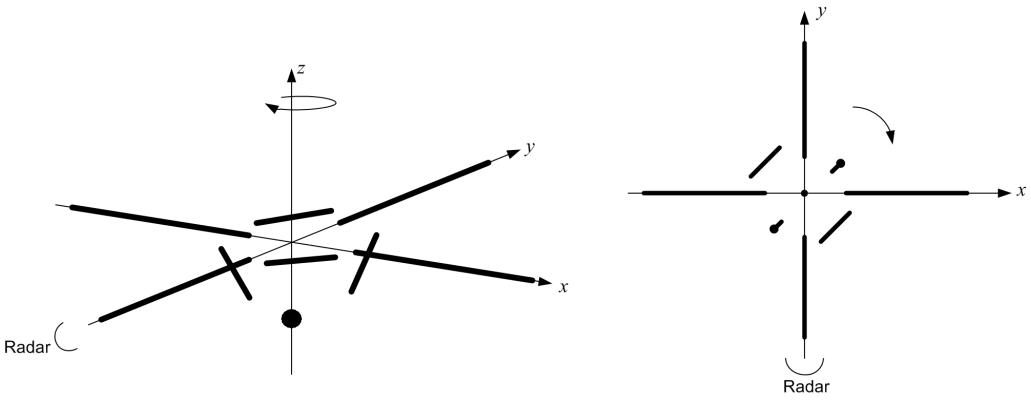

(a) An orthographic (left) and planar view (right) depicting the geometry of a more complex hypothetical helicopter rotor consisting of four rotating wires, two vertical rods and two horizontally oriented rods.

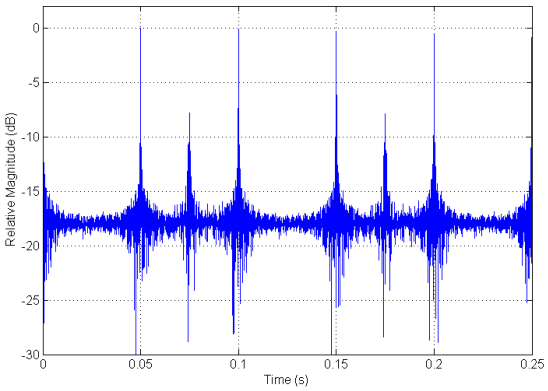

(b) Time-domain signal

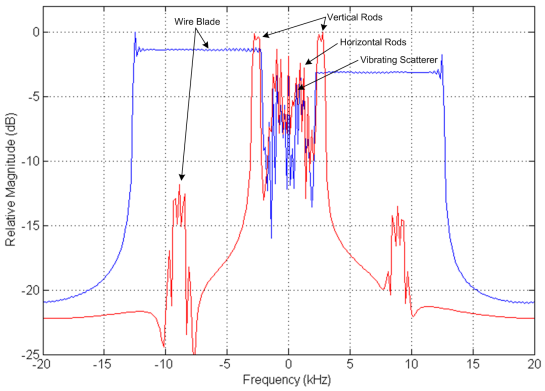

(c) Blade, vertical and horizontal rods flash spectra

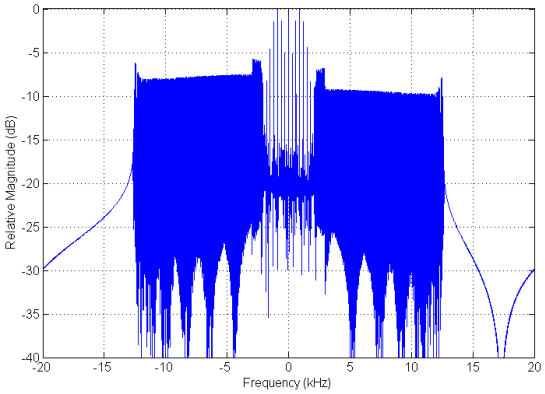

(d) Frequency-domain signal

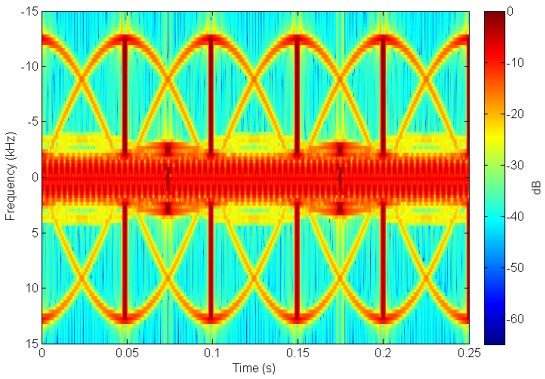

(e) Spectrogram

Figure 15: *Time and frequency plots of a simulated signal from a complex hypothetical helicopter illuminated by a 10 GHz radar with a PRF of 40 kHz. Plots normalised to peak signal.*

low frequency terms we highlight the blade signal. Figure 16(a) is the time-domain plot with low frequency filtering. The blade flash from the simulated data matches closely with the real data.

Figure 16(b) is the time-domain plot with high frequency filtering. Similarly, the blade return is suppressed and the rotor hub is highlighted. This plot shows the finer detail associated with the hub and the response from the different types of objects. The simulated and real data match closely using the objects to describe the rotor hub. Although there are features in the real data that are not reflected in the simulated data, the complexity of the hub structure makes it difficult to model everything.

For completeness, Figure 16(c) is the unfiltered time-domain signal showing the blade flash and rotor hub returns.

Figure 17(a) shows the spectra of a single blade from the simulated and real data. The general structure of the signal is comparable showing the single sided blade flash plateau and the tip Doppler. The length and cut-off point of this region is similar. The rotor hub features are also comparable with the region from -2 kHz to 0 kHz clearly showing a hub feature that is correctly modelled in the simulated data.

Figure 17(b) is the complete spectra of the simulated and real data. The general features of these plots include the complex hub region, the relative magnitudes of the positive and negative Doppler regions and the blade tip Doppler. This region, in particular, is highlighted and shown in Figure 17(c). The roll-off characteristics of the simulated signal closely compares with the real signal.

Considering the complexity of the rotor hub region, the overall similarities between the real and simulated signal is reasonably close.

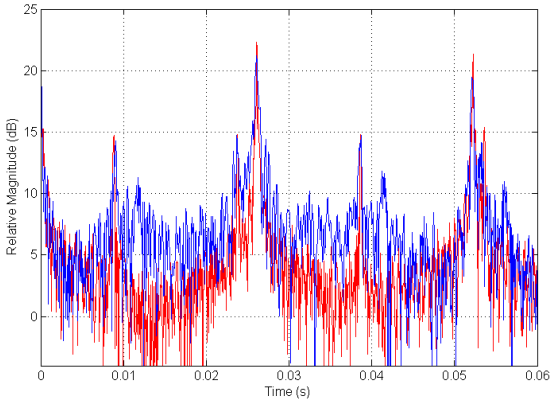

(a) Time-domain signal with low frequency components removed

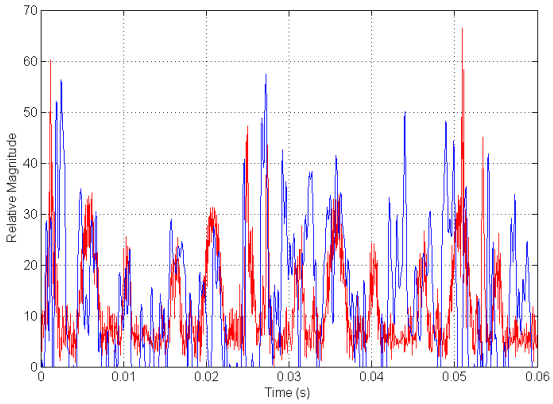

(b) Time-domain signal with high frequency components removed

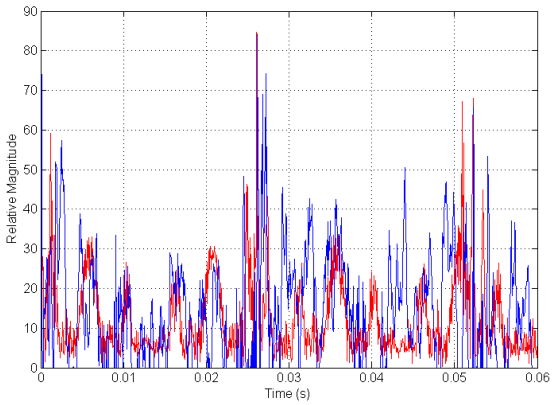

(c) Full time-domain signal

Figure 16: *Time-domain plots of the simulated signal (red) and real signal (blue) with high frequency filtering, low frequency filtering and no filtering.*

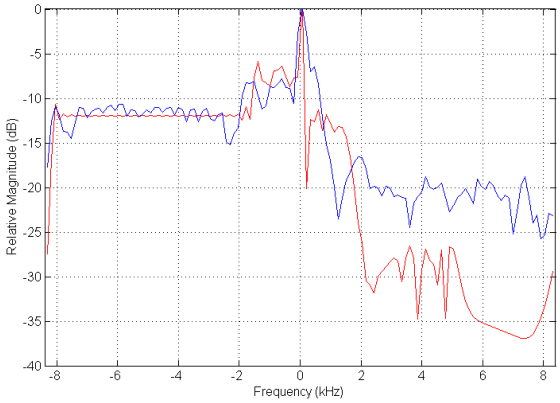

(a) Single blade flash spectra of simulated and real signal

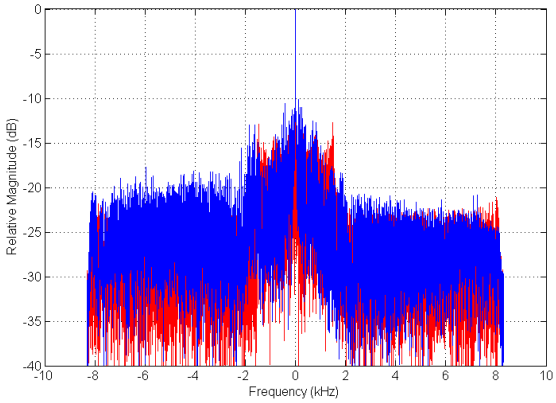

(b) Spectra of simulated and real signal

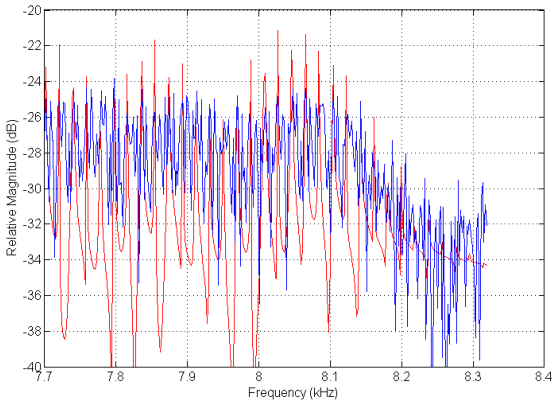

(c) Spectra of simulated and real signal around the tip Doppler

Figure 17: *Frequency-domain plots of the simulated signal (red) and real signal (blue) showing the flash spectra only, the full spectra and spectra zoomed around the tip Doppler. Plots normalised to peak signal.*

5 Discussion and Conclusion

We have presented a new and efficient tool for simulating a radar backscatter signal from a helicopter target, using a combination of newly reported closed-form solutions and simple numerical models. Relevant components of a helicopter are modelled by simple geometric objects, such as straight wires, rectangular plates and vibrating point scatterers. When combined to model an actual helicopter, the backscattered signal very closely resembles real data, as indicated in their time and frequency characteristics, without the overhead of numerically intensive computations.

To model a rotor blade more precisely using these simple objects, a straight wire with a reflectivity coefficient that varies along the blade length can be used, where this calculation is made using a one dimensional numerical integration, which gives more realistic results without increasing computational load. To model a rotor hub and helicopter body, we found that this can be efficiently achieved by using a collection of simple vertical and horizontal rods and using a number of vibrating point scatterers. Although only a limited number of rods were used to represent the hub, good agreement with real data has been demonstrated.

The collection of models presented provides a means to adequately simulate backscatter from a helicopter. Such a tool aides in the research and development of algorithms for detection and classification of helicopter targets.

Acknowledgements

We sincerely thank Dr. Andrew Shaw (Research Leader, Microwave Radar Branch) for his review, leadership, and the summer vacation student scholarship for Christopher Bourne, and also Dr. Leigh Powis (Head, Air-to-Air Radar Group) for his support.

References

1. Chen, V. & Ling, H., *"Time-Frequency Transforms for Radar Imaging and Signal Analysis"*, Artech House, Boston, 2002

2. Chen, V., Lin, C. & Pala, W., *"Time-Varying Doppler Analysis of Electromagnetic Backscattering From Rotating Object"*, IEEE Transactions, 2006

3. Whitrow,J., Cowley, W., *"An Analysis of the Radar Cross Section of Helicopter Rotors"*, DSTO Technical Report, ERL-0398-TR, February 1987, Confidential Classification.

4. Chen, V., Li, F., Ho, S. & Wechsler, H., *"Micro-Doppler Effect in Radar: Phenomenon, Model, and Simulation Study"*, IEEE Transaction, Aerospace and Electronic Systems, Vol. 42, No. 1, Jan. 2006.

5. Schneider, H., *"Application of an autoregressive reflection model for the signal analysis or radar echoes from rotating objects"*, IEEE Transaction, 1988.

6. Fliss, G., *"Tomographic radar imaging of rotating structures"*, in SAR: Proceedings of meeting SPIE conference, vol 1630, May 1992.

7. Boashash, B., *"Time-Frequency Signal Analysis and Processing: A Comprehensive Reference"*, Elsevier Publications, 2003.

8. Ruck, G. et al, *"Radar Cross Section Handbook"*, Vol 2, Plenum Press, NY, 1970.

9. Tait, P., *"Introduction to Radar Target Recognition"*, UK, IEE, 2005.

DISTRIBUTION LIST *

Modelling Helicopter Radar Backscatter

R. Melino, C. Bourne and H.T. Tran

AUSTRALIA

DEFENCE ORGANISATION	**No. of Copies**
Task Sponsor: DGAD	1 Printed
S&T Program	
Chief Defence Scientist Chief, Projects and Requirements Division DG Science Strategy and Policy	Doc. Data Sheet & Exec. Summary
Counsellor Defence Science, London	Doc. Data Sheet
Counsellor Defence Science, Washington	Doc. Data Sheet
Scientific Adviser to MRDC, Thailand	Doc. Data Sheet
Scientific Adviser Intelligence and Information	1
Navy Scientific Adviser	1
Scientific Adviser Army	1
Air Force Scientific Adviser	1
Scientific Adviser to the DMO	1
Scientific Adviser VCDF	Doc. Data Sheet & Dist. List
Scientific Adviser CJOPS	Doc. Data Sheet & Dist. List
Scientific Adviser Strategy	Doc. Data Sheet & Dist. List
Deputy Chief Defence Scientist Platform and Human Systems	Doc. Data Sheet & Exec. Summary
Chief of EWRD: Jackie Craig	Doc. Data Sheet & Dist. List
Research Leader RLMR: Andrew Shaw, EWRD	1
Head Air-to-Air Radar: Leigh Powis, EWRD	1
Author: Rocco Melino, EWRD	1 Printed
Author: Chris Bourne	1 Printed
Author: Hai-Tan Tran, EWRD	1 Printed
Cheng Anderson, EWRD	1
Deane Prescott, EWRD	1
James Morris, EWRD	1
Bevan Bates, EWRD	1
Brett Haywood, EWRD	1

DEFENCE SCIENCE AND TECHNOLOGY ORGANISATION DOCUMENT CONTROL DATA	1. CAVEAT/PRIVACY MARKING

2. TITLE	3. SECURITY CLASSIFICATION
Modelling Helicopter Radar Backscatter	Document (U) Title (U) Abstract (U)
4. AUTHORS	5. CORPORATE AUTHOR
R. Melino, C. Bourne and H.T. Tran	Defence Science and Technology Organisation PO Box 1500 Edinburgh, South Australia 5111, Australia

6a. DSTO NUMBER	6b. AR NUMBER	6c. TYPE OF REPORT	7. DOCUMENT DATE
DSTO–TR–2547	014–993	Technical Report	June, 2011

8. FILE NUMBER	9. TASK NUMBER	10. TASK SPONSOR	11. No. OF PAGES	12. No. OF REFS
2011/1029152/1	07/213	DGAD	28	9

13. URL OF ELECTRONIC VERSION	14. RELEASE AUTHORITY
`http://www.dsto.defence.gov.au/publications/scientific.php`	Chief, Electronic Warfare and Radar Division

15. SECONDARY RELEASE STATEMENT OF THIS DOCUMENT

Approved for Public Release

OVERSEAS ENQUIRIES OUTSIDE STATED LIMITATIONS SHOULD BE REFERRED THROUGH DOCUMENT EXCHANGE, PO BOX 1500, EDINBURGH, SOUTH AUSTRALIA 5111

16. DELIBERATE ANNOUNCEMENT

No Limitations

17. CITATION IN OTHER DOCUMENTS

No Limitations

18. DSTO RESEARCH LIBRARY THESAURUS

Helicopter radar backscatter, EM backscatter from rotating objects, Radar returns from rotating objects, Micro-Doppler effect, Time-domain analysis, Frequency-domain analysis, Time-frequency transforms, Helicopter modelling, Helicopter blades, Helicopter rotors, Rotor hubs.

19. ABSTRACT

This paper presents a study on the simulation of the radar backscatter signal from a helicopter in which the helicopter rotors, the helicopter rotor hub and helicopter body are modelled by an ensemble of straight wires, rods and rectangular plates in various orientations. Despite the simplicity of exact solutions used here, which give a significant advantage of very low computational cost, very good agreement with real data can be achieved.